

J.F. Booker and S. Boedo,

"Finite element analysis of elastic engine bearing lubrication: Theory",

Traitement des Problèmes de Lubrification par la Méthode des Eléments Finis,

Revue Européenne des Eléments Finis, Vol. 10, No. 6-7/2001, pp 705-724.

Finite Element Analysis of Elastic Engine Bearing Lubrication: Theory

J.F. Booker* — **S. Boedo****

** Sibley School of Mechanical and Aerospace Engineering
Cornell University
Upson Hall, Hoy Road, Ithaca, NY 14853 USA
j.f.booker@cornell.edu*

*** Department of Mechanical Engineering
Rochester Institute of Technology
76 Lomb Memorial Drive, Rochester, NY 14623 USA
sxbeme@rit.edu*

ABSTRACT: This paper reviews the theory of finite element mode-based elastohydrodynamic lubrication analysis (as applied in a companion paper to the bearing and structural design of a dynamically loaded automotive connecting rod).

RÉSUMÉ: La théorie présentée de l'analyse par la méthode des éléments finis des problèmes de lubrification élastohydrodynamique exprime les déformées élastiques dans une base modale. Cet article est accompagné d'un second qui applique le modèle à l'étude des paliers de bielle de moteur d'automobile sous chargement dynamique.

KEY WORDS: ehl, elastohydrodynamic, lubrication, modal, analysis, bearing

MOTS-CLÉS: ehl, lubrification, élastohydrodynamique, analyse, modal, palier

1. Introduction

This paper reviews the theory of finite element mode-based elastohydrodynamic lubrication (EHL) analysis (as applied in a companion paper [BOE 01] to the bearing and structural design of a dynamically loaded automotive connecting rod). As such, it does *not* attempt a general bibliographical review of the finite element method in lubrication, a task addressed elsewhere [BOU 01] in this special issue. Rather, it is limited to an outline of several decades of work by the authors and their colleagues, leading to their particular approach to problems of engine bearing lubrication analysis.

Engine bearing loading presents particular problems for lubrication analysis. The relatively high magnitude of loading introduces significant elastic deformation, while the rapid variation of loading makes conservation of mass in cavitating films a necessary analysis feature. Both features can be accommodated quite naturally via finite element analysis, bringing also the usual advantages of irregular meshes for irregular geometries. Modal analysis further allows a lower-order representation of structural displacement patterns, resulting in a robust and efficient simulation procedure which accommodates unrelated meshes for fluid and solid surfaces; as an additional potential benefit, modal interpretation of dynamic behavior may be of use in guiding structural design modifications [BOE 97b].

While engine bearing analyses typically concern *cylindrical* geometries, the methods described here have equally well been applied to *planar* [BOE 95a] and *spherical* geometries [KOT 95].

Presentation takes the form of a series of major sections covering related topics. Topics are introduced in 'bottom-up' order, starting with basic (distributed) relations of fluid and solid mechanics, followed by discretization via finite element analysis. Next, fluid/solid interaction (coupling) relations are introduced in discrete form, leading then to a discrete initial-boundary-value problem with algebraic constraints. Finally, this 'nodal' problem is replaced by a similar lower-order 'modal' problem through introduction of a constraining transformation to generalized coordinates.

The authors have elected an unusual mode of presentation, whereby each set of relations is presented *en bloc*, followed by an explanatory commentary.

2. Fluid

2.1. Mechanics

2.1.1. Mean motion: momentum & constitution

$$\langle \mathbf{u} \rangle = \underbrace{\langle \mathbf{u}^{a,b} \rangle}_{\text{Couette}} - \underbrace{(1/12)(h^2/\mu) \nabla p}_{\text{Poiseuille}} \quad [1]$$

with

$$\langle \mathbf{u}^{a,b} \rangle \equiv (\mathbf{u}^a + \mathbf{u}^b)/2 \quad [2]$$

2.1.2. Power dissipation

$$H = H_{\text{Couette}} + H_{\text{Poiseuille}} \geq 0 \quad [3]$$

with

$$H_{\text{Couette}} \equiv \int_A (\mu/h) \Delta \mathbf{u} \cdot \Delta \mathbf{u} \, dA \geq 0 \quad [4]$$

$$H_{\text{Poiseuille}} \equiv \int_A (1/12)(h^3/\mu) \nabla p \cdot \nabla p \, dA \geq 0 \quad [5]$$

with

$$\Delta \mathbf{u} \equiv \mathbf{u}^b - \mathbf{u}^a \quad [6]$$

2.1.3. Surface tractions

$$\boldsymbol{\tau}^a = -(\mu/h) \Delta \mathbf{u} + \nabla(ph/2) - p \nabla \langle z \rangle \quad [7]$$

$$\boldsymbol{\tau}^b = +(\mu/h) \Delta \mathbf{u} + \nabla(ph/2) + p \nabla \langle z \rangle \quad [8]$$

with mean surface position¹

$$\langle z \rangle \equiv (z^a + z^b)/2 \quad [9]$$

so

$$\boldsymbol{\tau}^a + \boldsymbol{\tau}^b = \nabla(ph) \quad [10]$$

¹ Mean surface position is everywhere zero for a mid-film coordinate system [BOO 89].

2.1.4. *Areal density: definition*

$$\rho^* \equiv \rho h \quad [11]$$

2.1.5. *Lineal flux: definition*

$$\mathbf{f} \equiv \rho h \langle \mathbf{u} \rangle \equiv \rho^* \langle \mathbf{u} \rangle \quad [12]$$

2.1.6. *Continuity: mass conservation*

$$\int_S \mathbf{n} \cdot \mathbf{f} \, dS + (\int_A \rho^* \, dA)_t = 0 \quad [13]$$

2.1.7. *Commentary*

Figure 1 shows solid bearing surfaces 'a' and 'b' separated by a fluid film of thickness h.

Figure 2 shows an *arbitrary* cylindrical section of fluid film, its projection onto the x-y reference plane, and 2-D mass flux and normal vectors on its boundary.

Figure 3 again shows the 2-D quantities in the x-y plane.

Detailed derivations of relations [1-13] are available elsewhere [BOO 89]. All vector quantities therein are 2-D, lying in the x-y reference plane.

Derivation of mean fluid velocity relation [1] reflects equilibrated flow of a purely viscous (inertialess) fluid between impervious surfaces without slip. Though the full derivation is complex, all but the constant value can be inferred by dimensional analysis considerations. Such purely viscous 'creeping' flows consist only of surface ('Couette') and pressure gradient ('Poiseuille') driven components, as seen in both the equation of motion [1] and the power dissipation relations [3-5].

Surface tractions [7,8] act *on* fluid surfaces 'a' and 'b' as indicated.

Relatively unfamiliar *areal* (as contrasted with *volumetric*) mass density [11] and *lineal* (as opposed to *areal*) mass flux [12] are appropriate for thin film analysis.

Mass conservation relation [13] implies impervious surfaces 'a' and 'b' .

2.2. Mathematical forms

2.2.1. Continuity: integral (weak) form

$$\int_{\Lambda} (\nabla \cdot \mathbf{f} + \rho^*_{,t}) dA = 0 \quad [14]$$

2.2.2. Continuity: differential (strong) form

$$\nabla \cdot \mathbf{f} + \rho^*_{,t} = 0 \quad [15]$$

2.2.3. Continuity: integral (weighted) form

$$\int_{\Lambda} \phi (\nabla \cdot \mathbf{f} + \rho^*_{,t}) dA = 0 \quad [16]$$

2.2.4. Combination: continuity & motion (Reynolds equation)

$$\begin{aligned} \nabla \cdot (h^2/12) (\rho^*/\mu) \nabla p &= \rho^*_{,t} + \nabla \cdot \rho^* \langle \mathbf{u}^{a,b} \rangle \\ &\text{diffusion} \quad \text{unsteady} \quad \text{steady (convection/entrainment)} \\ &= \rho^*_{,t} + \nabla \rho^* \cdot \langle \mathbf{u}^{a,b} \rangle + \rho^* \nabla \cdot \langle \mathbf{u}^{a,b} \rangle \\ &\quad \text{squeeze} \quad \text{wedge} \quad \text{stretch} \end{aligned} \quad [17]$$

or

$$\begin{aligned} \nabla \cdot (h^3/12) (\rho/\mu) \nabla p &= (\rho h)_{,t} + \nabla \cdot (\rho h) \langle \mathbf{u}^{a,b} \rangle \\ &= \rho h_{,t} + h \rho_{,t} \quad \text{squeeze} \\ &\quad + \rho \nabla h \cdot \langle \mathbf{u}^{a,b} \rangle + h \nabla \rho \cdot \langle \mathbf{u}^{a,b} \rangle \quad \text{wedge} \\ &\quad + \rho h \nabla \cdot \langle \mathbf{u}^{a,b} \rangle \quad \text{stretch} \end{aligned} \quad [18]$$

2.2.5. Functional (augmented)

$$\begin{aligned} J &= 1/2 \int_{\Lambda} (h^2/12) (\rho^*/\mu) \nabla p \cdot \nabla p \, dA \\ &\quad - \int_{\Lambda} \rho^* \langle \mathbf{u}^{a,b} \rangle \cdot \nabla p \, dA + \int_{\Lambda} \rho^*_{,t} p \, dA \\ &\quad + \int_{S_f} \mathbf{f} \cdot \mathbf{n} p \, dS \end{aligned} \quad [19]$$

2.2.6. *Commentary*

Continuity forms [14-16] evidently derive directly from [13] through application of the divergence theorem, noting that the region of integration is *arbitrary*.

The Reynolds equation is of such great importance in lubrication analysis that alternate forms [17,18] are shown and their terms appropriately identified. (It should be noted that the labeled 'stretch' term is negligible for ordinary bearings.)

The augmented functional [19] corresponding to [17] is a common starting point for approximate solutions.

2.3. *Distributed problem formulation*

2.3.1. *Boundary conditions*

$$\text{boundary } S_p : \quad p \quad \text{'essential'} \quad [20]$$

$$\text{boundary } S_f : \quad \mathbf{f} \cdot \mathbf{n} \quad \text{'natural'} \quad [21]$$

with

$$S = S_p \cup S_f \quad [22]$$

where S_p is non-vanishing.

2.3.2. *Boundary-value problem*

Satisfy combined field equation [17/18] with respect to pressure distribution p meeting *both* conditions [20] and [21].

2.3.3. *Variational problem*

Minimize augmented functional [19] with respect to pressure distribution p meeting *only* condition [20], thus meeting condition [21] *naturally*.

(The two problem formulations are formally equivalent [BOO 72].)

2.4. Discrete relations

2.4.1. Variational method

$$\begin{aligned}
 J = & \frac{1}{2} \int_{\Lambda} (h^2/12) (\rho^*/\mu) \nabla p \cdot \nabla p \, dA \\
 & - \int_{\Lambda} \rho^* \langle \mathbf{u}^{a,b} \rangle \cdot \nabla p \, dA + \int_{\Lambda} \rho^*_{,t} p \, dA \\
 & + \int_{S_f} \mathbf{f} \cdot \mathbf{n} p \, dS
 \end{aligned} \tag{19}$$

with

$$p = \sum N_i p_i \tag{23}$$

gives

$$J = \frac{1}{2} \sum \sum p_i F_{ij} p_j - \sum q_i p_i - \sum q_i^c p_i \tag{24}$$

so

$$\partial J / \partial p_i = 0$$

gives

$$\sum F_{ij} p_j = q_i + q_i^c \tag{25}$$

with

$$F_{ij} = \int_{\Lambda} (h^2/12) (\rho^*/\mu) \nabla N_i \cdot \nabla N_j \, dA \tag{26}$$

$$q_i = - \int_{S_f} \mathbf{f} \cdot \mathbf{n} N_i \, dA \tag{27}$$

$$q_i^c = q_i^u + q_i^{\hat{\rho}^*} \tag{28}$$

with

$$q_i^u = \int_{\Lambda} \rho^* \langle \mathbf{u}^{a,b} \rangle \cdot \nabla N_i \, dA \tag{29}$$

$$q_i^{\hat{\rho}^*} = - \int_{\Lambda} \rho^*_{,t} N_i \, dA \tag{30}$$

2.4.2. Weighted residual (Galerkin) method

$$\int_{\Lambda} \phi (\nabla \cdot \mathbf{f} + \rho^*_{,t}) \, dA = 0 \tag{16}$$

with

$$p = \sum N_i p_i \tag{23}$$

$$\phi = \sum N_i \phi_i \tag{31}$$

gives essentially the same result [24-29].

2.4.3. Alternate forms

$$F_{ij} = \int_{\Lambda} (h^3/12) (\rho/\mu) (N_{i,x} N_{j,x} + N_{i,y} N_{j,y}) dA \quad [32]$$

$$q_i^e = q_i^{ux} + q_i^{uy} + q_i^{\hat{h}} + q_i^{\hat{\rho}} \quad [33]$$

with

$$q_i^{ux} = \int_{\Lambda} \rho h \langle u^{x,a,b} \rangle N_{i,x} dA \quad [34]$$

$$q_i^{uy} = \int_{\Lambda} \rho h \langle u^{y,a,b} \rangle N_{i,y} dA \quad [35]$$

$$q_i^{\hat{h}} = - \int_{\Lambda} \rho h_{,t} N_i dA \quad [36]$$

$$q_i^{\hat{\rho}} = - \int_{\Lambda} h \rho_{,t} N_i dA \quad [37]$$

so if

$$\rho_{,t} = \sum N_j D\rho_j \quad [38]$$

$$h_{,t} = \sum N_j Dh_j \quad [39]$$

$$\langle u^{x,a,b} \rangle = \sum N_j \langle u^{x,a,b} \rangle_j \quad [40]$$

$$\langle u^{y,a,b} \rangle = \sum N_j \langle u^{y,a,b} \rangle_j \quad [41]$$

then

$$q_i^{ux} = (\sum \int_{\Lambda} \rho h N_{i,x} N_j dA) \langle u^{x,a,b} \rangle_j = Q_{ij}^{ux} \langle u^{x,a,b} \rangle_j \quad [42]$$

$$q_i^{uy} = (\sum \int_{\Lambda} \rho h N_{i,y} N_j dA) \langle u^{y,a,b} \rangle_j = Q_{ij}^{uy} \langle u^{y,a,b} \rangle_j \quad [43]$$

$$q_i^{\hat{h}} = - (\sum \int_{\Lambda} \rho N_i N_j dA) Dh_j = Q_{ij}^{Dh} Dh_j \quad [44]$$

$$q_i^{\hat{\rho}} = - (\sum \int_{\Lambda} h N_i N_j dA) D\rho_j = Q_{ij}^{D\rho} D\rho_j \quad [45]$$

with

$$Q_{ij}^{ux} = \int_{\Lambda} \rho h N_{i,x} N_j dA \quad [46]$$

$$Q_{ij}^{uy} = \int_{\Lambda} \rho h N_{i,y} N_j dA \quad [47]$$

$$Q_{ij}^{Dh} = - \int_{\Lambda} \rho N_i N_j dA \quad [48]$$

$$Q_{ij}^{D\rho} = - \int_{\Lambda} h N_i N_j dA \quad [49]$$

2.4.4. Commentary

Nodal flows q_i and q_i^e are here defined by [27-30] as positive *inward* (in direct opposition to the commonly applied lubrication convention [BOO 72]), thus ensuring that fluidity matrix F_{ij} is here *positive* semidefinite (and singular). This break with tradition has the effect of bringing the form of lubrication equations into alignment with analogous ones from other fields (e.g., conductive heat transfer).

Interpolations [23, 38-41] require shape functions for specific elements. Appendix A.1 provides a family of such functions for the commonly-used 3-node linear triangular elements suggested by Figure 4.

Further detail requires specification of the behavior of functions h , ρ , μ . Appendix A.2 provides resulting matrices for these 3-node linear triangular elements with linearly interpolated h and uniform ρ , μ .

2.5. Discrete problem formulation

2.5.1. Pressure-flow relation

Supposing full knowledge of fluidity matrix F_{ij} and equivalent flows q_i^e , a typical problem consists of n relations

$$\Sigma F_{ij} p_j = q_i + q_i^e \quad [25]$$

with n complementary knowns/unknowns p_i , q_i .

Since *either* pressure p_i *or* flow q_i (but not both) is known for each node, solution follows standard methods of finite element analysis for 'mixed' problems.

For example, pressure p_i is typically known for external boundary nodes, while flow q_i is typically known (zero) for internal nodes.

Positive values of flows q_i and q_i^e inspire *positive* shifts in pressure p_i .

2.5.2. *Work-equivalent nodal forces*

Similarly

$$\int_A p h_{,t} dA = \Sigma r_i D h_i \quad [50]$$

with

$$p = \Sigma N_j p_j \quad [51]$$

$$h_{,t} = \Sigma N_i D h_i \quad [52]$$

gives

$$\Sigma A_{ij} p_j = r_i \quad [53]$$

with

$$A_{ij} \equiv \int_A N_i N_j dA \quad [54]$$

2.5.3. *Nodal kinematics*

$$d_i \equiv h_i - c_i \quad [55]$$

2.5.4. *Nodal equation of motion*

$$\Sigma C_{ij} D d_j + b_i = - r_i \quad [56]$$

2.5.4.1. *Commentary*

Explicit expressions for damping C_{ij} and static force b_i can be obtained (with some effort) through combining relations [25], [33], [42-45], [53], [55], [56] with specified nodal q_i , p_i .

(As seen below, symbolic evaluation of these coefficients is not always required.)

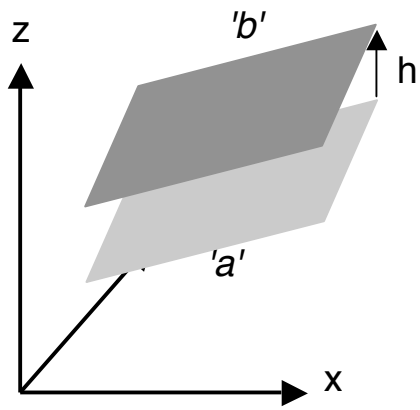


Figure 1.

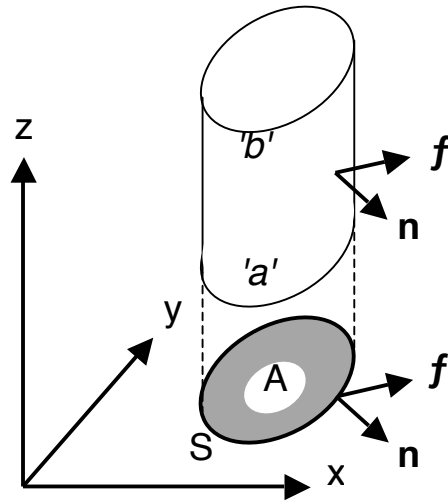


Figure 2.

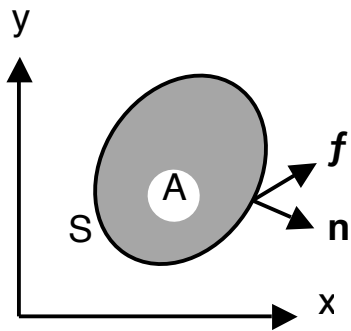


Figure 3.

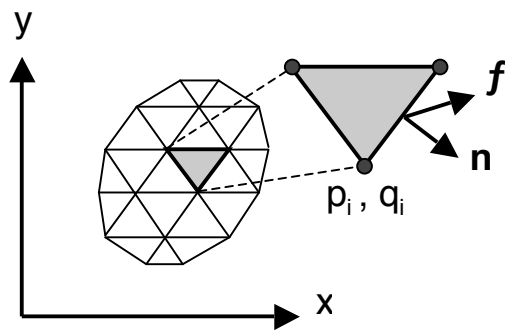


Figure 4.

2.6. Cavitation

2.6.1. Mechanics

2.6.1.1. Dynamic (mass-conserving)

$$\begin{aligned}
 (p - p_{\text{cav}}) (\rho_{\text{liq}} - \rho) &= 0 \\
 p_{\text{cav}} &\leq p \\
 0 &\leq \rho \leq \rho_{\text{liq}} \\
 \mu / \mu_{\text{liq}} &= \rho / \rho_{\text{liq}}
 \end{aligned}
 \tag{57}$$

2.6.1.2. Quasi-static

$$\begin{aligned}
 \rho &= \rho_{\text{liq}} \\
 p_{\text{cav}} &\leq p \\
 0 &\leq \rho_{\text{liq}} \\
 \mu &= \mu_{\text{liq}}
 \end{aligned}
 \tag{58}$$

2.6.1.3. Commentary

The distributed and discrete fluid models above can be extended to address cavitation through treating the fluid film as a *mixture* of incompressible liquid and fully compressible vapor (of negligible density and viscosity). The liquid/vapor demarcation is assumed to be 2-dimensional.

Figure 5(a) illustrates the abrupt (non-analytic) pressure-density relations [57] assumed for the fluid mixture, while Figure 5(b) illustrates reduced relations [58] for a pure liquid.

2.6.2. Problem formulation

The distributed boundary-value problem given above is simply augmented by initial specification of mixture density to form an *initial*-boundary-value problem.

2.6.3. Problem solution

The presumed scenario of cavitation under this mixture model is 3-fold:

Initiation occurs instantaneously when pressure drops locally to its cavitation value, whereupon mixture density *begins* to drop from liquid value as vapor *begins* to form.

Evolution of cavitation, once initiated, proceeds temporally at cavitation pressure and declining and/or increasing mixture density. (Transport in fixed-pressure cavitated zones is driven entirely by the 'Couette' term of equation [1].)

Reformation occurs instantaneously wherever mixture density rises to liquid value, whereupon pressure is no longer fixed at cavitation pressure.

Discrete cavitation algorithms can be built upon quasi-static relation [25] when initial values of mixture density ρ_i at internal nodes are specified initially and then integrated forward over time ([KUM 90b], [KUM 91a,b,c], [LAB 85], [BOE 95a]², etc.)

At any one node, 1 of 3 variables (pressure p_i , flow q_i , equivalent flow $q_i^{\rho_i}$) is always unknown (though iteration may be necessary to determine *which* one). For example, suppose that the fluid film is initially entirely liquid and that boundary nodes have fixed pressure (greater than cavitation value) and null density rate flow; for boundary nodes the unknown variable is flow. At any one interior node flow is null, pressure is greater than/equal to cavitation value, and density rate equivalent flow is greater than/equal to zero; iteration with quasi-static relation [25] determines a consistent pairing of nodal pressure and density rate equivalent flow. (Nodal density rate is then determined from density rate equivalent flow.)

If nodal density rates are used to integrate nodal density values forward in time, the resulting '*dynamic*' algorithm is mass-conserving; if nodal density is maintained at its liquid value, the resulting '*quasi-static*' algorithm is *not* mass-conserving.

² Such 'normal separation' studies are much more general than may be supposed, since the (arbitrary) x-y reference frame can always be chosen in such a way that *observed* mean tangential surface motion vanishes.

3. Solid

3.1. Discrete relations

Structural solids follow the conventional relations of quasi-static linear elasticity embodied in commercial software and expressed in discretized form as

$$\Sigma K_{ij} d_j = r_i + r_i^e \quad [59]$$

where equivalent nodal forces r_i^e encompass external load, body forces, etc. Because displacements d_i are *relative*, stiffness K_{ij} and forces r_i must be derived from their more conventional counterparts (based on *absolute* displacements); detailed formulas for such derivations are available [KUM 90, BOE 97a, BOE 00]. It should be noted that stiffness matrix K_{ij} is always singular, since *rigid body* relative displacements d_i must be allowed.

4. Fluid-solid system

4.1. Discrete relations

4.1.1. Fluid

$$\underline{\underline{C}}(\underline{\underline{d}},t) D\underline{\underline{d}} + \underline{\underline{b}}(\underline{\underline{d}},t) = -\underline{\underline{r}}(t) \quad [56]$$

4.1.2. Solid

$$\underline{\underline{K}} \underline{\underline{d}} = \underline{\underline{r}} + \underline{\underline{r}}^e \quad [59]$$

4.1.3. Commentary

Singly subscripted variables are represented by singly underlined bold symbols, and doubly subscripted variables are represented by doubly underlined bold symbols.

- Vector $\underline{\underline{c}}$ and matrices $\underline{\underline{A}}$ and $\underline{\underline{K}}$ are considered fixed system parameters.
- Vector $\underline{\underline{b}}$ and matrix $\underline{\underline{C}}$ are known functions of $\underline{\underline{d}}$ (and t).
- Vector $\underline{\underline{b}}$ and matrix $\underline{\underline{C}}$ depend on matrices $\underline{\underline{A}}$, $\underline{\underline{E}}$, and $\underline{\underline{Q}}^e$.
- Vector $\underline{\underline{r}}^e$ is a known function of t .
- Matrices $\underline{\underline{A}}$, $\underline{\underline{K}}$, and $\underline{\underline{C}}$ are square and symmetric (iffi ρ is uniform).
- Matrix $\underline{\underline{A}}$ is nonsingular, while both $\underline{\underline{K}}$ and $\underline{\underline{C}}$ are singular.

Relations [56], [59] appear variously [KUM 89,90], [KOT 95], [BOE 97a,b], etc. (These relations can be considered generalizations of other relations developed for a very simple prototypical application [BOO 84].)

4.2. Modal problem

4.2.1. Kinematic constraint transformation

$$\underline{\mathbf{d}} = \underline{\mathbf{T}} \underline{\mathbf{d}}' \quad [60]$$

4.2.2. Constrained solid

$$\underline{\mathbf{K}}' \underline{\mathbf{d}}' = \underline{\mathbf{r}}' + \underline{\mathbf{r}}^{e'} \quad [61]$$

where

$$\underline{\mathbf{K}}' = \underline{\mathbf{T}}^T \underline{\mathbf{K}} \underline{\mathbf{T}} \quad [62]$$

$$\underline{\mathbf{r}}' = \underline{\mathbf{T}}^T \underline{\mathbf{r}} \quad [63]$$

$$\underline{\mathbf{r}}^{e'} = \underline{\mathbf{T}}^T \underline{\mathbf{r}}^e \quad [64]$$

4.2.3. Constrained fluid

$$\underline{\mathbf{C}}'(\underline{\mathbf{d}}',t) D\underline{\mathbf{d}}' + \underline{\mathbf{b}}'(\underline{\mathbf{d}}',t) = -\underline{\mathbf{r}}'(t) \quad [65]$$

where

$$\underline{\mathbf{C}}' = \underline{\mathbf{T}}^T \underline{\mathbf{C}} \underline{\mathbf{T}} \quad [66]$$

$$\underline{\mathbf{b}}' = \underline{\mathbf{T}}^T \underline{\mathbf{b}} \quad [67]$$

$$\underline{\mathbf{r}}' = \underline{\mathbf{T}}^T \underline{\mathbf{r}} \quad [63]$$

4.2.4. Constrained fluid-solid system

$$\underline{\mathbf{C}}'(\underline{\mathbf{d}}',t) D\underline{\mathbf{d}}' + \underline{\mathbf{b}}'(\underline{\mathbf{d}}',t) + \underline{\mathbf{K}}' \underline{\mathbf{d}}' = \underline{\mathbf{r}}^{e'}(t) \quad [68]$$

or

$$D\underline{\mathbf{d}}' = \underline{\mathbf{C}}'^{-1} (\underline{\mathbf{r}}^{e'} - \underline{\mathbf{b}}' - \underline{\mathbf{K}}' \underline{\mathbf{d}}') \quad [69]$$

4.2.5. *Commentary*

Due account is taken of forces of constraint in forming the transformations.

The chief motivation for the transformations is reduction in system order. Owing to the (normally radically) reduced order of the modal representation, *numerical* determination of the coefficients $\underline{\mathbf{c}}'$ and $\underline{\mathbf{b}}'$ via [56] is conventional. However, additional advantages accrue. For example, generalized coordinates $\underline{\mathbf{d}}'$ may themselves be more intuitively meaningful than nodal displacements $\underline{\mathbf{d}}$.

In principle, transformation $\underline{\mathbf{T}}$ could be selected in a wide variety of ways. Discrete (nodal) versions of distributed orthogonal functions would be attractive, allowing quite seamlessly for unrelated separate meshes on fluid and solid surfaces. On the other hand, if $\underline{\mathbf{T}}$ satisfies the general eigenproblem [BOE 95b]

$$\underline{\mathbf{T}}^T \underline{\mathbf{K}} \underline{\mathbf{T}} = \underline{\mathbf{T}}^T \underline{\mathbf{A}} \underline{\mathbf{T}} \underline{\mathbf{A}} \quad [70]$$

where matrix $\underline{\mathbf{A}}$ is a diagonal 'spectral' matrix of (unknown) eigenvalues, then $\underline{\mathbf{K}}'$ and $\underline{\mathbf{A}}'$ are diagonal, and the resulting transformation $\underline{\mathbf{T}}$ is mesh-invariant (in the sense that the basic *shape* of modes is invariant). This common approach also allows relatively easily for unrelated separate meshes on fluid and solid surfaces following a *single* (static) translation of $\underline{\mathbf{T}}$ from solid to fluid mesh representation. An example of a transformation mode family obtained in this fashion is illustrated in the companion paper [BOE 01]. There the eigenmode shapes are shown in order of their corresponding eigenvalues, progressing from rigid body modeshapes (corresponding to null eigenvalues) to successively more complex elastic modes, usually (though not always) occurring in rough pairs. (It can be shown formally that the ordering of suitably normalized eigenmode shapes by modal strain energy is equivalent to ordering by their eigenvalues.)

No matter how the transformation mode family may finally be calculated, a judicious *selection* from it is necessary to obtain desired reduction in system order. As demonstrated in the companion paper [BOE 01], the selection process can be approached iteratively, adding higher modes until apparent numerical convergence. Fortunately, the selection process need only be performed once for a particular design. (If only rigid body modes are selected, analysis reduces to one for rigid surfaces.)

Whatever modes are selected, modal displacements (generalized coordinates) contained in $\underline{\mathbf{d}}'$ are specified initially and then numerically integrated forward in time according to the system ODE [69]. In the event that dynamic cavitation is to be considered, fluid mixture density ρ must be followed in time as well.

See [KUM 89], [KUM 90a], [BOE 95b], [BOE 97a] for details of this modal formulation and [OLS 97], [OLS 01] for details of a variation not covered here.

6. Nomenclature

6.1. Distributed variables

t	time	[T]
x,y,z	spatial coordinates	[L]
D	temporal derivative (total)	[T ⁻¹]
$,t$	temporal derivative (partial)	[T ⁻¹]
∇	spatial derivative	[L ⁻¹]
A	area	[L ²]
S	boundary	[L]
\mathbf{n}	unit outward normal	[-]
h	thickness	[L]
c	clearance	[L]
d	displacement	[L]
μ	viscosity	[FL ⁻² T]
ρ	volumetric mass density	[ML ⁻³]
ρ^*	areal mass density	[ML ⁻²]
\mathbf{f}	lineal mass flux	[ML ⁻¹ T ⁻¹]
\mathbf{u}	fluid velocity	[LT ⁻¹]
$\mathbf{u}^a, \mathbf{u}^b$	surface velocities	[LT ⁻¹]
$\langle z \rangle$	surface position average	[L]
$\langle \mathbf{u} \rangle$	fluid velocity average	[LT ⁻¹]
$\langle \mathbf{u}^{a,b} \rangle$	surface velocity average	[LT ⁻¹]
$\Delta \mathbf{u}$	surface velocity difference	[LT ⁻¹]
p	pressure	[FL ⁻²]
$\boldsymbol{\tau}$	surface traction	[FL ⁻²]
J	functional	[F ² L ⁻³ T]
H	power dissipation	[FLT ⁻¹]
ϕ	weight function	[-]
N_i	shape function	[-]

6.2. Discrete variables

i, j, k	node index	[-]
n	node total	[-]
F_{ij}	fluidity	[LT]
Q_{ij}	fluidity	[various]
q_i	flow	[MT ⁻¹]
q_i^e	equivalent flow	[MT ⁻¹]
C_{ij}	damping	[FL ⁻¹ T]
K_{ij}	stiffness	[FL ⁻¹]
b_i	static force	[F]
r_i	force	[F]
r_i^e	equivalent force	[F]
T_{ij}	transformation	[L] ³
Λ_{ii}	eigenvalue	[FL ⁻³]

³ Dimensions shown correspond to case of *dimensionless* modal displacements (generalized coordinates).

Bibliography/References

- [BOE 95a] BOEDO S., BOOKER J.F.,
"Cavitation in normal separation of square and circular plates",
ASME Journal of Tribology, vol. 117 no. 3, 1995, p. 403-410.
- [BOE 95b] BOEDO S., BOOKER J.F., WILKIE M.J.,
"A mass conserving modal analysis for elastohydrodynamic lubrication",
Proc. 21st Leeds-Lyon Symposium on Tribology: Lubricants and Lubrication,
1995, Elsevier, p. 513-523.
- [BOE 95c] BOEDO S., BOOKER J.F.,
"Body force and surface roughness effects
in a mass-conserving mode-based elastohydrodynamic lubrication model",
Proc. Japan International Tribology Conference, 1995.
- [BOE 97a] BOEDO S., BOOKER J.F.,
"Surface roughness and structural inertia
in a mode-based mass-conserving elastohydrodynamic lubrication model",
ASME Journal of Tribology, vol. 119 no. 3, 1997, p. 449-455.
- [BOE 97b] BOEDO S., BOOKER J.F.,
"Mode stiffness variation in elastohydrodynamic bearing design",
Proc. 23rd Leeds-Lyon Symposium on Tribology:
Elastohydrodynamics - Fundamentals and Applications of Lubrication and Traction,
1997, Elsevier, p. 685-697, 740-741.
- [BOE 00] BOEDO S., BOOKER J.F.,
"A mode-based elastohydrodynamic lubrication model with elastic journal and sleeve",
ASME Journal of Tribology, vol. 122 no. 1, 2000, p. 94-102.
- [BOE 01] BOEDO S., BOOKER J.F.,
"Finite element analysis of elastic engine bearing lubrication: Application",
Revue Européenne des Eléments Finis, vol. xx no. x, 2001, p. xx-xx.
- [BOO 72] BOOKER J.F., HUEBNER K.H.,
"Application of finite-element methods to lubrication: an engineering approach",
ASME Journal of Lubrication Technology, vol. 94 no. 4, 1972, p. 313-323.
Errata: Vol. 98, No. 1, January 1976, p. 39.

- [BOO 84] BOOKER J.F., SHU C.F.,
 "Finite element analysis of transient elasto-hydrodynamic lubrication",
 Proc. 10th Leeds-Lyon Symposium on Tribology:
 Developments in Numerical and Experimental Methods Applied to Tribology,
 1984, Butterworths, p. 157-163.
- [BOO 89] BOOKER J.F.,
 "Basic equations for fluid films with variable properties",
 ASME Journal of Tribology, vol. 111 no. 3, 1989, p. 475-483.
- [BOU 01] BOU-SAÏD B.,
 "La méthode des éléments finis en lubrification: une revue bibliographique",
 Revue Européenne des Eléments Finis, vol. xx no. x, 2001, p. xx-xx.
- [EID 76] EIDELBERG B.E., BOOKER J.F.,
 "Application of finite element methods to lubrication:
 squeeze films between porous surfaces",
 ASME Journal of Lubrication Technology, vol. 98 no. 1, 1976, p. 175-180,186.
- [GOE 80] GOENKA P.K., BOOKER J.F.,
 "Spherical bearings: static and dynamic analysis via the finite element method",
 ASME Journal of Lubrication Technology, vol. 102 no. 3, 1980, pp. 308-319.
- [GOE 83] GOENKA P.K., BOOKER J.F.,
 "Effect of surface ellipticity on dynamically loaded cylindrical bearings",
 ASME Journal of Lubrication Technology, vol. 105 no. 1, 1983, p. 1-12.
- [KOT 95] KOTHARI M., BOOKER J.F., BARTEL D.L.,
 "Analysis of artificial hip joints as spherical bearings",
 Proc. 21st Leeds-Lyon Symposium on Tribology: Lubricants and Lubrication
 1995, Elsevier, p. 93-98.
- [KUM 89] KUMAR A., BOOKER J.F., GOENKA P.K.,
 "Dynamically loaded journal bearings: a modal approach to EHL design analysis",
 Proc. 15th Leeds-Lyon Symposium on Tribology:
 Tribological Design of Machine Elements,
 1989, Elsevier, p. 305-315, 508-510.
- [KUM 90a] KUMAR A., GOENKA P.K., BOOKER J.F.,
 "Modal analysis of elastohydrodynamic lubrication: a connecting rod application",
 ASME Journal of Tribology, vol. 112 no. 3, 1990, p. 524-534.

- [KUM 90b] KUMAR A., BOOKER J.F.,
"Cavitation and thermal effects in journal bearing applications",
Proc. Japan International Tribology Conference, 1990, p. 1491-1496.
- [KUM 91a] KUMAR A., BOOKER J.F.,
"A finite element cavitation algorithm",
ASME Journal of Tribology, vol. 113 no. 2, 1991, p. 276-286.
- [KUM 91b] KUMAR A., BOOKER J.F.,
"A finite element cavitation algorithm: application/validation",
ASME Journal of Tribology, vol. 113 no. 2, 1991, p. 255-261.
- [KUM 91c] KUMAR A., BOOKER J.F.,
"Mass-conservative cavitation analysis for engine bearings",
Proc. 17th Leeds-Lyon Symposium on Tribology: Vehicle Tribology
1991, Elsevier, p. 27-32.
- [KUM 94] KUMAR A., BOOKER J.F.,
"A mass and energy conserving finite element lubrication algorithm",
ASME Journal of Tribology, vol. 116 no. 4, 1994, p. 667-671.
- [LAB 85] LABOUFF G.A., BOOKER J.F.,
"Dynamically loaded journal bearings:
a finite element treatment for rigid and elastic surfaces",
ASME Journal of Tribology, vol. 107 no. 4, 1985, p. 505-515.
- [OLS 97] OLSON E.G., BOOKER J.F.,
"A finite element treatment of hydrodynamically lubricated journal bearings
with structural inertia and elasticity",
Proc. 23rd Leeds-Lyon Symposium on Tribology:
Elastohydrodynamics - Fundamentals and Applications of Lubrication and Traction,
1997, Elsevier, p. 661-673.
- [OLS 01] OLSON E.G., BOOKER J.F.,
"EHD Analysis with Distributed Structural Inertia",
ASME Journal of Tribology, vol. 123 no. 3, 2001, p. 462-468.

Appendix A. 3-node triangular element

Reference: [BOO 72]

A.1. Shape functions

A typical element has 3 nodes numbered (consecutively) counterclockwise and 3 linear shape (interpolation) functions

$$N_i(x,y) = (a_i + b_i x + c_i y) / (2A) \quad [A1]$$

orthonormalized such that

$$N_i(x_j, y_j) = \delta_{ij} \quad [A2]$$

so that more generally

$$\sum N_i(x,y) = 1 \quad [A3]$$

Setting (arbitrarily)

$$2A = a_1 + a_2 + a_3 \quad [A4]$$

the required coefficients are thus

$$\begin{array}{lll} a_1 = x_2 y_3 - x_3 y_2 & b_1 = y_2 - y_3 & c_1 = x_3 - x_2 \\ a_2 = x_3 y_1 - x_1 y_3 & b_2 = y_3 - y_1 & c_2 = x_1 - x_3 \\ a_3 = x_1 y_2 - x_2 y_1 & b_3 = y_1 - y_2 & c_3 = x_2 - x_1 \end{array} \quad [A5]$$

Differentiation gives

$$\begin{array}{l} N_{i,x} = b_i / (2A) \\ N_{i,y} = c_i / (2A) \end{array} \quad [A6]$$

while integration gives

$$\langle N_1^l N_2^m N_3^n \rangle \equiv (1/A) \int N_1^l N_2^m N_3^n dA = 2/l! m! n! / (2+l+m+n)! \quad [A7]$$

A.2. Fluid matrices

If
$$h = \sum N_j h_j \quad [A8]$$

$\rho, \mu = \text{uniform} \quad [A9]$

then
$$A_{ij} = (1 + \delta_{ij}) A / 12 \quad [A10]$$

$$F_{ij} = (\rho/\mu) \langle h^3 \rangle (b_i b_j + c_i c_j) / (48A) \quad [A11]$$

$$Q_{ij}^{ux} = \rho b_i f_j / 24 \quad [A12]$$

$$Q_{ij}^{uy} = \rho c_i f_j / 24 \quad [A13]$$

$$Q_{ij}^{Dh} = -\rho (1 + \delta_{ij}) A / 12 \quad [A14]$$

$$Q_{ij}^{D\rho} = -G_{ij} A / 60 \quad [A15]$$

with
$$f_j = \sum h_k (1 + \delta_{kj}) = \sum h_k + h_j = 3 \langle h \rangle + h_j \quad [A16]$$

$$G_{ij} = \sum h_k [(1 + \delta_{ij}) + (\delta_{ik} + \delta_{kj})^2]$$

$$= 3 \langle h \rangle (1 + \delta_{ij}) + 2 \sum h_k \delta_{ik} \delta_{kj} + h_i + h_j \quad [A17]$$

with
$$\langle h \rangle = \sum h_k / 3 \quad [A18]$$

$$\langle h^3 \rangle = (\sum h_k \sum h_k^2 + \Pi h_k) / 10 \quad [A19]$$

with indicated sums and products over

$$k = 1 \text{ to } 3 \quad [A20]$$